New & Renewable Energy 2025. 9 Vol. 21, No. 3
ISSN 1738-3935 (Print)
ISSN 2713-9999 (Online)
https://doi.org/10.7849/ksnre.2025.0006

[2025-9-ST-001]

Validation Methods for Oscillating Motion in Large-Scale Oscillating Heat Pipes for Solar Water Heaters

Il Yoon*

Received 5 February 2025 **Revised** 9 June 2025 **Accepted** 2 July 2025 **Published online** 29 August 2025

ABSTRACT Solar thermal energy is particularly advantageous for heating purposes because of its higher efficiency compared with photovoltaic energy. Oscillating heat pipes (OHPs) can further enhance the efficiency of solar thermal systems. The effectiveness of OHPs depends on the oscillating motion of the working fluid inside the tubes. While validating the oscillating motion is important, its direct visual validation is challenging owing to the large scale of the system. Therefore, developing indirect methods to confirm the presence of oscillating motion in large-scale OHPs is essential. In this study, a solar water heater utilizing three sets of large-scale OHPs was fabricated and tested. The temperature and efficiency data were compared with previously validated data from a small-scale reference OHP that exhibited temperature changes synchronized with the oscillatory motion. The analysis was focused on general trends, such as temperature fluctuation patterns and efficiency changes, rather than on direct numerical equivalence. The results suggest that a sudden temperature drop or cessation of the temperature rise indicates the onset and continuation of the oscillating motion. Additionally, a sudden increase in efficiency serves as another indicator. Lastly, a periodic temperature fluctuation suggests continuation of the oscillating motion after its initiation.

Key words Oscillating heat pipe(진동형히트파이프), Solar water heater(태양열온수기), Oscillating motion(진동운동), Visualization (시각화), Validation(검증)

Nomenclature

A : area [m^2]
c : specific heat capacity at constant pressure [J/kg·K]
$I(t)$: solar irradiance [W/m^2]
$\dot{m}$: mass flow rate [kg/s]
q : heat transfer rate [W]
R : thermal resistance [K/W]
T : temperature [°C] or [K]
η : efficiency

Subscript

c : condenser
e : evaporator
HE : heat exchanger
i : inlet
o : outlet
p : constant pressure (used in cp)

1. Introduction

As climate change becomes a more serious issue, wider use of renewable energy is inevitable.[1] One of the most common ways to utilize renewable energy is

Assistant Professor, Department of Global Industry, Jeonju Kijeon College
***Corresponding author:** yoonengineer@jk.ac.kr
Tel: +82-63-280-5208

through solar energy. While photovoltaic technology is more widely used than solar thermal energy, solar thermal energy is more efficient for heating buildings. One way to improve the performance of a solar water heater is by utilizing an oscillating heat pipe (OHP). An OHP is a promising thermal device for transferring heat from the hot side to the cold side. Research indicates that, under specific conditions, OHPs outperform conventional heat pipes, which consist of a single closed tube with an internal wicking structure. While OHP technology has primarily been studied for electronics cooling applications, it also shows great potential for use in solar water heaters.

An OHP consists of three sections: the evaporator, the condenser, and the adiabatic section. Heat is introduced at the evaporator, transported through the adiabatic section, and subsequently dissipated at the condenser. The capillary tubes are filled with a working fluid, with the filling ratio varying based on the experimental setup. When heat is applied to the evaporator, a pressure difference develops between the evaporator and the condenser, prompting the working fluid to oscillate between these two regions. Numerous studies have been conducted to visualize the oscillating motion of working fluid in OHPs, and comprehensive reviews are available.[2,3] The studies in these reviews directly validated active oscillating motion by capturing images of working fluid movement.

Due to the high heat transfer rate of an OHP, it can efficiently transfer heat from a solar collector to a heat exchanger or heat storage unit in a solar water heater. The use of OHPs in solar water heaters has been explored by numerous research groups. While these studies highlight the advantages that OHPs offer in improving solar water heater performance, the dimensions of OHPs used in solar water heater applications are generally larger than those used in visualization studies. Table 1 shows the lengths of OHPs used for solar water heaters and those used in visualization studies. In general, the OHPs used for solar water heaters are significantly longer than those used for visualization studies.

Since the key factor in determining the performance of solar water heaters with OHPs is the onset and continuation of oscillating motion in the OHPs, it is important to validate that actual oscillating motion occurs in the OHPs of solar water heaters to ensure good performance. While oscillating motion in small-scale OHPs has been validated visually by capturing images of working fluid movement, oscillating motion in OHPs used for solar water heaters has not been

Table 1. Lengths of OHPs used for solar water heaters and visualization studies

OHPs used for solar water heaters	Length [mm]
Wang *et al.*, 2022 [4]	190
Aref *et al.*, 2021 [5]	1,250
Charoensawan *et al.*, 2021 [6]	1,000
Winarta *et al.*, 2019 [7]	720
Zhao *et al.*, 2018 [8]	990
Gao *et al.*, 2018 [9]	2,000
Xu *et al.*, 2017 [10]	500
More *et al.*, 2016 [11]	1,400
Kim *et al.*, 2013 [12]	2,660
	2,725
	2,547
Yang *et al.*, 2009 [13]	1,500
Rittidech *et al.*, 2009 [14]	1,850
Rittidech *et al.*, 2007 [15]	2,500
Average	1,559
OHP used for visualization studies	**Length [mm]**
Bao *et al.*, 2023 [16]	255
Patel *et al.*, 2019 [17]	565
Liu *et al.*, 2016 [18]	400
Rittidech *et al.*, 2012 [19]	300
Wilson *et al.*, 2011 [20]	155
Borgmeyer *et al.*, 2010 [21]	254
Bhuwakietkumjohn *et al.*, 2010 [22]	200
Lips *et al.*, 2010 [23]	570
Soponpongpipat *et al.*, 2009 [24]	300
Kim *et al.*, 2003 [25]	220
Tong *et al.*, 2001 [26]	160
Average	307

visually validated. This is likely because direct visualization of large-scale OHPs is challenging. Therefore, it is valuable to explore indirect validation methods for detecting oscillating motion in large-scale OHPs used in solar water heaters.

In this study, a solar water heater with three large-scale OHPs was fabricated and installed outdoors for testing. The test data were compared with temperature and neutron imaging data from a relatively small-scale OHP previously built and tested by a research group that the author was part of.[27] For convenience, this relatively small-scale OHP, which was used for neutron imaging, is referred to as the small-scale OHP in this paper. By comparing the data from the OHPs used in the solar water heater and the small-scale OHP, this study investigated whether the onset of oscillating motion in the OHPs of the solar water heater could be validated by observing temperature behavior and efficiency changes. Given the differences in OHP scale, working fluid properties, and operating conditions, a direct numerical comparison is not feasible. Instead, the results are compared in terms of qualitative trends, such as the presence of sudden temperature drops, efficiency increases, and periodic fluctuations, which indicate oscillating motion. Additionally, the study examined whether the continuation of oscillating motion could be validated by analyzing temperature patterns.

2. Fabrication and Experimental Setup

2.1 Fabrication

2.1.1 System components and functioning

The solar water heater was designed and fabricated by dividing it into four main components: the solar collector, heat exchanger, water tank, and supporting structure. A schematic illustration of the system is presented in Fig. 1. The heater operates as follows:

a. Solar panels absorb sunlight, heating up in the process.

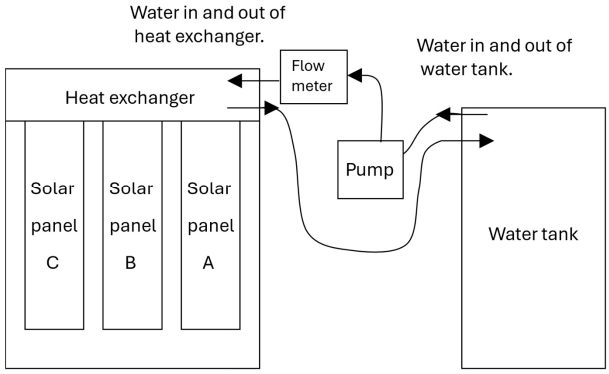

Fig. 1. Schematic of the solar water heater

b. Heat from the solar panels is transferred to the heat sinks within the heat exchanger via the oscillating motion of the working fluid in the oscillating heat pipe (OHP) tubes.
c. Water is pumped from the tank through a hose into the heat exchanger.
d. The water circulates through the heat exchanger, passing over the heat sinks to absorb heat.
e. The heated water is then returned to the tank via another hose.

2.1.2 Solar collector

The solar collector consisted of three sets of solar panels, each equipped with back insulation plates, double-paned glass covers, and insulated edge walls. Each solar panel incorporated a six-turn OHP made from copper tubes sandwiched between aluminum straps. The decision to fabricate six-turn OHPs was based on a reference OHP for which neutron imaging and synchronized temperature data were available.[27,28] Acetone was selected as the working fluid because it initiated oscillatory motion at a relatively lower heat input and exhibited more vigorous oscillations, resulting in better thermal performance compared to water under the same heat input.[28]

The dimensions of each tube segment were 237 mm × 1,145 mm, with inner and outer diameters of 1.65

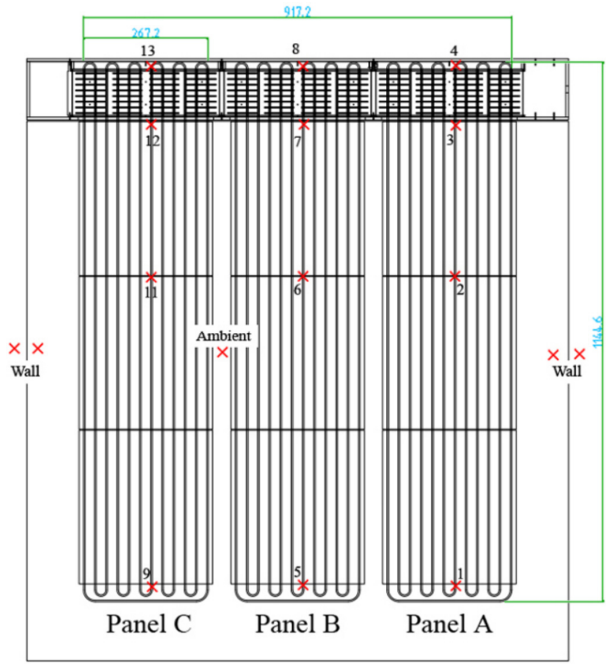

Fig. 2. Dimensions of OHPs and positions of thermocouples attached to the surfaces of OHPs. Each thermocouple is represented by a numbered red "x"

mm and 3.18 mm, respectively. The aluminum straps were painted with selective black paint to maximize absorption in the visible and infrared light spectrum. Detailed dimensions of the OHP are shown in Fig. 2. Solar irradiance was measured using an SP-110-SS pyranometer (Apogee Instruments, USA), with a sensitivity of 0.2 mV per $W \cdot m^{-2}$ and a calibration uncertainty of less than 3% at 1,000 $W \cdot m^{-2}$. Measurements were recorded at one-second intervals.

2.1.3 Heat exchanger

The OHP sets were inserted into a heat exchanger made up of six aluminum heat sinks attached to aluminum plates. The ends of the OHP tube segments were positioned between these aluminum plates. The outer casing of the heat exchanger was constructed from acrylic, providing transparency for visual inspection and ease of machining. Accessibility was prioritized in the design, allowing the front wall to open via draw latches, enabling easy access for maintenance or modifications. Fiberglass insulation wrapped around the heat exchanger improved thermal performance, as shown in Fig. 3.

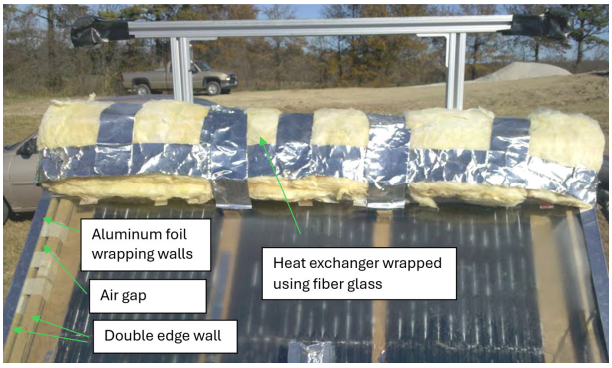

Fig. 3. The fabricated edge walls and heat exchanger wrapped with fiberglass insulation

2.1.4 Water tank and measurement devices

A 208-liter water tank was used, filled with 170 liters of deionized water. The tank was insulated with fiberglass and wrapped in aluminum foil to minimize heat loss. A flow meter (FTB-1411, Omega) was installed between the tank outlet and the heat exchanger inlet to monitor flow rates. The FTB-1411 operates within a flow range of 0.6 to 3.0 GPM (2.3 to 11.3 LPM) and provides a K-factor of 18,000 pulses per gallon. Flow rate data were recorded at one-second intervals. The accuracy of the flow meter is ±1% of reading over the upper 70% of its measuring range.

2.1.5 Material and thermal properties

The solar panels were covered with double-paned glass, offering an R-value of 0.50 $m^2 \cdot K/W$. Beneath the glass, a hardboard with a thermal conductivity of 0.14 $W/m \cdot K$ and a thickness of 3.176 mm was placed. Three layers of fiberboard (each 12.7 mm thick, R-value of 0.23 $m^2 \cdot K/W$) were positioned beneath the hardboard. All components were supported on an aluminum structure.

2.1.6 Double edge walls

The double edge walls were made from two fiberboard layers with a 10 mm air gap in between for improved insulation. The walls measured 38.1 mm in height, with a thickness of 18.5 mm, and were wrapped with 0.1 mm aluminum foil. A fabricated edge wall is shown in Fig. 3.

2.2 Experimental setup

The experimental setup, including the heat exchanger and three solar panels, is schematically illustrated in Fig. 1. Selective black paint was applied to the aluminum straps of the solar panels to absorb the visible and infrared wavelengths that carry most of the radiant energy. The fabricated solar panels and heat exchanger, prior to the installation of double-paned glass and double edge walls, are shown in Fig. 4.

2.2.1 Working fluid and filling ratios

The filling ratio is one of the factors that determine the performance of an OHP. Many studies have researched the effects of the filling ratio, and comprehensive review papers are available.[2,29] In general, a low filling ratio can lead to dry-out because there is insufficient working fluid in an OHP tubing to be evaporated. Conversely, if the filling ratio is too high, there may not be enough vapor space to generate sufficient vapor pressure to initiate and maintain the oscillatory motion. Therefore, determining the optimal filling ratio is critical, as it directly influences the thermal performance of the solar water heater. However, identifying the optimal filling ratio requires considerations of many factors, such as the geometry of an OHP, inclination, etc. Therefore, it is hard to determine the optimal filling ratio without actual testing. In general, filling ratios between 20% and 80% are considered acceptable for acetone as a working fluid, according to various studies. However, the effect of varying the filling ratio is not within the scope of this study, as the focus is on validating oscillatory motion and its impact on performance.

Fig. 4. Solar panels and heat exchanger. Selective black paint was applied to the surface of the panels. Thermocouples were attached to the positions indicated in Fig. 2. The glass and edge walls were not installed at this point.

Acetone was used as the working fluid for the oscillating heat pipes (OHPs) in this study. The target filling ratio for all OHPs was 80%. Due to unfamiliarity with the OHP fabrication process, a high filling ratio was chosen to compensate for potential fluid loss during fabrication. However, the final measured filling ratios were 73.0%, 80.5%, and 80.7% for the OHPs in panels A, B, and C, respectively, due to challenges in precisely filling the liquid into the OHP tubes. Although the filling ratio of the OHP in panel A deviated more from the intended value compared to those in panels B and C, this did not affect the results of this study, as the data from panel A was excluded due to low vacuum status. When dismantling the OHP tubes after testing, panels B and C produced a clear hissing sound when cutting, indicating a sudden air influx and confirming the presence of sufficient vacuum. In contrast, panel A produced only a relatively weak hissing sound compared to panels B and C, suggesting a lower vacuum level. Although the data from panel A was excluded, the results from panels B and C are sufficient for validation, as they can be cross-compared for consistency. Although

the low vacuum level in the tube of panel A may have reduced the performance of the solar water heater, this is acceptable, as the purpose of this study is not to evaluate the heater's performance but to propose methods for validating both the onset and continuation of oscillating motion in the OHPs used in the system.

2.2.2 Temperature monitoring

T-type thermocouples (Omega) with an accuracy of ±1.0°C or ±0.75% above 0°C, and ±1.0°C or ±1.5% below 0°C, were used to record temperature data at various points across the system. Their placements were configured as shown in Fig. 2, where each thermocouple is represented by a numbered red "x". The positions include:

- Panels: Thermocouples were attached to the surface of each panel to monitor temperature.
- Heat Exchanger and Water Tank: Thermocouples were installed at the inlet and outlet of the heat exchanger and the water tank to measure temperature changes.
- Side Walls: Two thermocouples were attached to each wall—one on the interior surface and one on the exterior—to measure heat loss through the walls.
- Glass: Four thermocouples were positioned on the double-paned glass—two on the inside and two on the outside—to assess heat loss through the glass.
- Back Plate: To evaluate heat loss through the hardboard and fiberboard, two thermocouples were attached to the inner surface of the hardboard within the collector, and two were placed on the outer surface of the back plate.

2.2.3 Testing conditions

Experiments were conducted on sunny or mostly sunny days. Occasionally, clouds caused shading, which affected panel temperatures. The solar panels were oriented southward and tilted at a 45-degree angle to maximize solar energy collection.

2.2.4 Data acquisition

Thermocouple temperature readings were measured using a National Instruments SCXI-1600 data acquisition system, which has a maximum uncertainty of ±0.2°C. The acquisition interval was set at 1/100 seconds for temperature measurements. Taking both factors of data acquisition and T-type thermocouples into account, the overall measurement uncertainty was estimated to be within approximately ±1.2°C, ensuring the consistency and reliability of the observed temperature data.

2.2.5 Construction of space-time diagrams from neutron images

The detailed experimental setup and analysis methods for the small-scale reference OHP, which provide previously validated data for this study, are available.[27] To visualize the dynamic behavior of two-phase flow in the oscillating heat pipe (OHP), a spatiotemporal image processing technique was applied to neutron radiography data.[30] Each frame was processed to extract a one-dimensional brightness profile along the curved flow path. This was achieved by digitally straightening the bent tube geometry, beginning from the middle position of the long connecting leg at the condenser side, which is the connector located between thermocouple 23 and 24 in Fig. 1 of a reference work,[27] and continuing through the entire loop. The resulting profiles, which reflect neutron attenuation (and thus phase distribution along the tube), were stacked horizontally in chronological order to generate a two-dimensional space-time diagram. Fig. 5 (b) presents a representative space-time diagram. In this diagram, the vertical axis represents position along the tube, while the horizontal axis denotes time, expressed as frame index. Darker regions correspond to liquid slugs (high neutron attenuation), while brighter areas indicate vapor plugs. The darker regions on the left appear as bands, indicating static liquid slugs. Over time, these transit into streaks, representing active motion of the slugs. In this way,

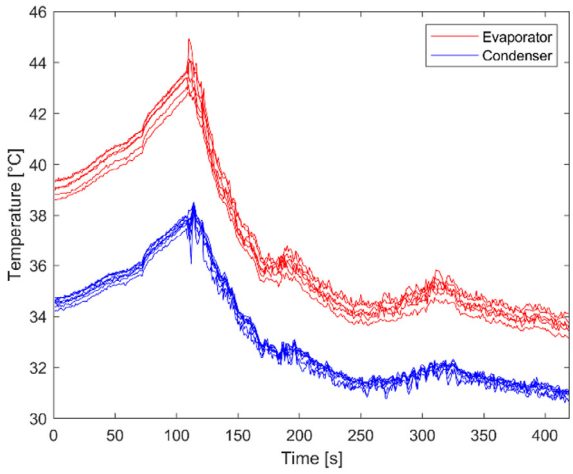

(a)

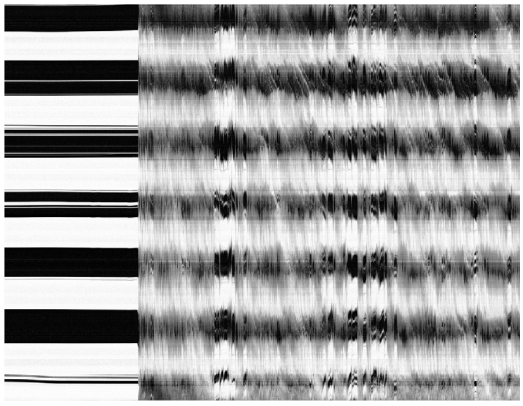

(b)

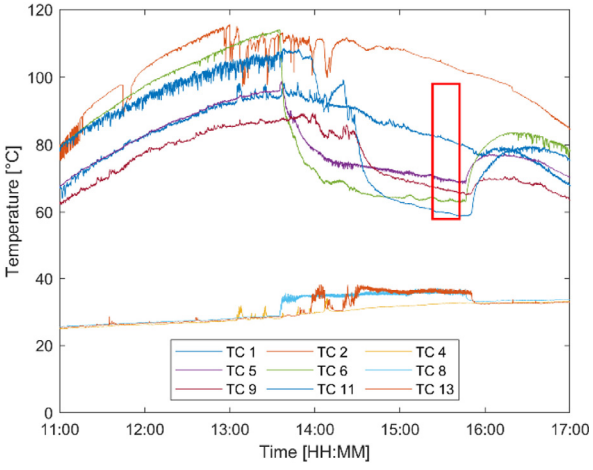

(c)

Fig. 5. (a) Temperature responses of the evaporator and condenser sections in the small-scale OHP. (b) Corresponding spatiotemporal diagram constructed from neutron images of the small-scale reference OHP. Dark regions represent liquid slugs, while bright regions correspond to vapor plugs. (c) Temperature changes in the OHP used for the solar water heater.

the space-time diagrams reveal oscillatory motion, flow regime transitions, and slug-plug dynamics within the OHP.[30]

3. Results and Discussion

Utilizing OHPs to improve the performance of a solar water heater is a topic worth studying. However, the dimensions of OHPs that can be used for solar water heaters are relatively larger than those that have been widely studied, which are smaller in size. Due to their relatively larger size, the working conditions required to initiate and maintain oscillatory motions differ from those of small-scale OHPs. This means that it is not guaranteed that oscillatory motions will readily occur in larger OHPs used in solar water heaters, as they do in smaller-scale ones. Therefore, it is important to validate that liquid slugs actively oscillate in OHPs used in solar water heaters. In this section, three validation methods are proposed to confirm oscillatory motion in OHPs used in solar water heaters: (1) a sudden temperature drop or the cessation of temperature increase in the evaporator, (2) sudden increases in efficiency, and (3) periodic temperature fluctuations synchronized with oscillatory motion. These indicators provide indirect yet strong evidence of oscillatory motion, helping to validate the performance of large-scale OHPs where direct visualization is challenging.

Before discussing further, it is worth mentioning that a direct numerical comparison between large-scale OHPs and small-scale OHPs is not appropriate. The scale of the OHP affects the frequency and amplitude of oscillating motion, and differences in working fluid properties influence the onset of oscillations. Therefore, while this study draws insights from previously validated small-scale OHP data, the comparison remains qualitative rather than absolute, ensuring that any conclusions account for these influencing factors.

3.1 Sudden temperature drops on the evaporator

An OHP is a heat transfer device that transports heat from the evaporator (heating section) to the condenser (cooling section) through the oscillating motion of a working fluid within a vacuumed tube. This oscillation is driven by pressure differences between vapor plugs in the evaporator and condenser. When heat is applied to the evaporator, the pressure difference increases, causing the nearly static liquid slugs to suddenly begin oscillating. This sudden movement results in an abrupt and enhanced transfer of heat from the evaporator to the condenser, leading to a sudden temperature drop at the evaporator.

In an OHP used in a solar water heating system, as solar intensity increases, heat is absorbed in the evaporator, causing a rise in temperature and evaporation of the working fluid. This leads to pressure differences between the evaporator and condenser. When a sufficient pressure difference develops, the liquid slugs suddenly begin to oscillate actively and continue their motion. As a result of this active oscillation, the heat accumulated in the evaporator is suddenly transferred to the condenser, leading to a sudden temperature drop in the evaporator.

Fig. 5 (a) shows that there are sudden temperature drops in the evaporator and condenser of the small-scale OHP at around 120 seconds, while the temperatures were previously increasing. From observations of image data, liquid slugs in the OHP begin to oscillate actively at this point. This means that temperatures increase steadily before active oscillation begins and then decrease steeply once oscillation starts. This suggests that active oscillation triggers sudden temperature drops. The OHP in the solar water heater shows similar sudden temperature drops at the evaporator at around 1:40 PM for panel B (TC 5 and TC 6) and at 2:00 PM and 2:30 PM for panel C (TC 9 and TC 11). This indirectly indicates that liquid slugs begin to actively oscillate at around these times in panels B and C, even though oscillatory motion cannot be observed directly. Therefore, this temperature behavior can be used to validate oscillatory motion in an OHP used for solar water heaters.

On the other hand, the evaporator temperature of panel A does not show any sudden temperature drop, although it exhibits gentle temperature fluctuations between 1:00 PM and 2:30 PM. This suggests that either oscillatory motion did not occur or it was very weak in panel A. A possible cause is an undetected leak in the tube, which would have led to a lower vacuum level. This was confirmed during dismantling: when the tube was cut, it produced only a very weak hissing sound, in contrast to the clear hissing sounds observed when cutting the tubes of panels B and C. While the condenser temperature also shows a sudden decrease in the small-scale OHP, the OHPs in the solar water heater instead show sudden increases in temperature at the same time the evaporator temperature suddenly decreases. This is the opposite behavior compared to the condenser temperature changes in the small-scale OHP. This difference is likely due to the rate of heat transfer from the condenser to the cold reservoir. When the liquid slugs oscillate actively, a large amount of heat is transferred from the evaporator to the condenser. From there, the heat is dissipated to the cold reservoir via water convection on the surface of the condenser. As shown in Fig. 6, the relative size of the condenser in the solar water heater OHP is much smaller than that in the small-scale OHP. This implies that a relatively large amount of heat is transferred into the condenser from the evaporator, while only a relatively small amount is removed from the condenser to the cold reservoir. This imbalance causes a temporary accumulation of heat in the condenser, resulting in a sudden temperature rise in the condenser of the large-scale OHP, which is similar to a bottleneck effect. In contrast, the condenser in the small-scale OHP is able to effectively and immediately dissipate heat to the cold reservoir due to its relatively large size, which causes a sudden

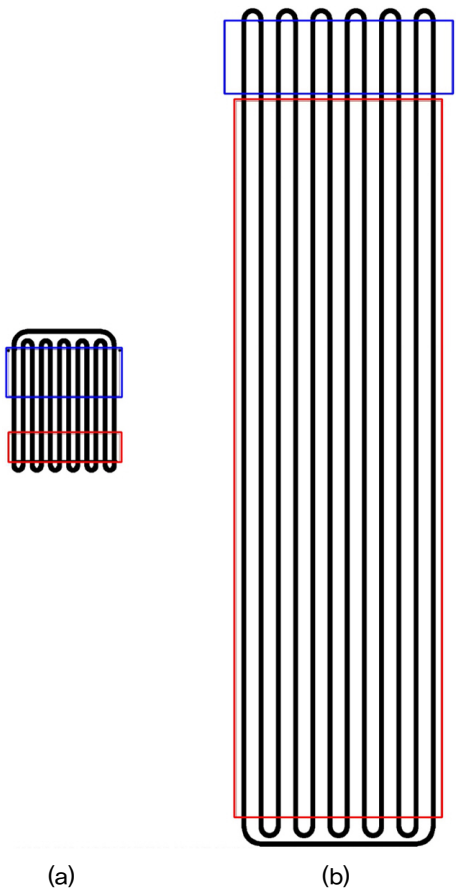

Fig. 6. Relative size comparison between the small-scale reference OHP and the OHP used for the solar water heater. (a) The small-scale reference OHP with available neutron imaging and synchronized temperature data. (b) The large-scale OHP fabricated for the solar water heater system in this study.

temperature drop.

Studies conducted by other research groups also report sudden temperature changes at the onset of oscillatory motion. For example, the study by Wang *et al.*[4] shows that temperature increases steadily until oscillatory motion begins. In Figure 8 of Wang *et al.*,[4] the temperature suddenly stops increasing and begins to fluctuate when oscillation starts which is shown in the green dotted box. The study by Winarta *et al.*[7] also reports a steady temperature increase followed by a sudden transition to fluctuations or drop, with no further increase as long as the heat input remains constant, as illustrated in Figures 2 and 3 of their study for T11. The study by Xu *et al.*[10] also presents similar temperature behavior, as illustrated in Fig. 4 of their study for T4. Therefore, a sudden temperature change—whether a sudden drop or a sudden stop in temperature increase—is synchronized with the onset of oscillatory motion. This can serve as a validation method for detecting oscillatory motion in OHPs used in solar water heaters. One might wonder what conditions cause a sudden temperature drop and what conditions cause a stop in temperature increase. Although this was not considered in this study because it is beyond the scope, it is a topic worth investigating in future research.

3.2 Sudden efficiency increases

A sudden change in the efficiency of a solar water heater utilizing OHPs can serve as an additional method to validate the occurrence and continuation of oscillatory motion. The efficiency of the system used in this study is determined using the following equation,[31]

$$\eta = \frac{q}{I(t)A} \tag{1}$$

where q is determined by the following equation,[31]

$$q = \dot{m} c_p (T_{o,HE} - T_{i,HE}) \tag{2}$$

The efficiency graph in Fig. 7 (a) shows sudden increases, which are synchronized with sudden temperature changes. At around 13:40, efficiency suddenly increases as the evaporator temperature of panel B suddenly decreases. At around 14:10, another sudden efficiency increase is observed as the evaporator temperature of panel C drops. Since sudden temperature drops in the evaporator are caused by the onset of active oscillatory motion, the sudden increase in efficiency is also presumably caused by the onset of oscillatory motion. Therefore, a sudden increase in efficiency is another indicator of the onset of oscillatory

motion in OHPs used in solar water heaters. One important point is that oscillatory motion is a key factor in the performance of solar water heaters with OHPs. The data show that efficiency increases significantly once liquid slugs begin oscillating actively. This highlights the importance of ensuring oscillatory motion for better performance in solar water heaters with OHPs. Thus, it is critical to initiate oscillatory motion and maintain it for as long as possible. It is suggested that future studies focus on identifying conditions that facilitate the initiation and maintenance of oscillatory motion.

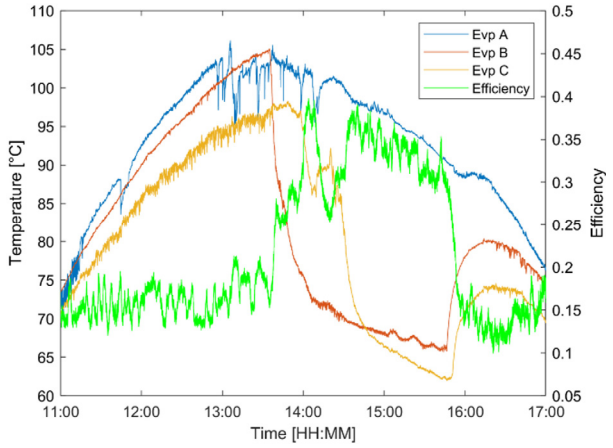

(a)

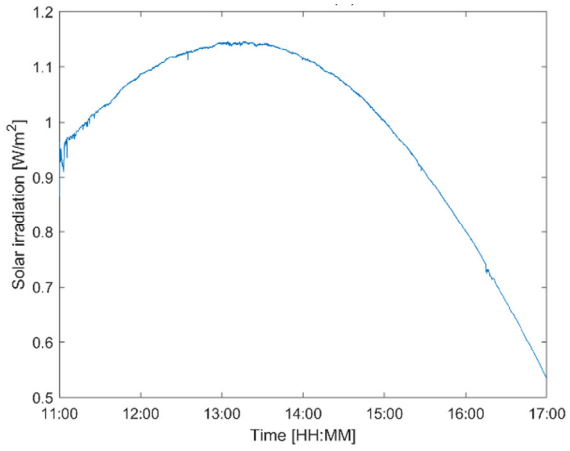

(b)

Fig. 7. (a) Sudden increases in thermal efficiency are observed, particularly around 13:30–14:40. (b) The corresponding solar irradiance during the same period is shown for reference.

3.3 Periodical temperature fluctuation synchronized with oscillatory motion

Fig. 8 shows the temperature changes of the small scale OHP recorded by thermocouples 4 and 5, along with the position changes of a liquid slug as it oscillates near these thermocouple locations. This demonstrates the thermal coupling between internal two-phase oscillations and external wall temperature response. It shows that temperatures fluctuate periodically when the liquid slug passes the points where the thermocouples are attached to the outer surface of the tube. The data clearly indicate that these temperature fluctuations are synchronized with the oscillatory motion of the liquid slug. Additionally, the frequency of temperature fluctuations matches the frequency of the oscillatory motion of the liquid slug. From the observation of image data, temperature fluctuations at a thermocouple do not always occur when a liquid slug passes the point where the thermocouple is attached. However, when periodic temperature fluctuations are present, they are always associated with oscillatory motion. In other words, the presence of periodic temperature fluctuations confirms the existence of oscillatory motion. Therefore, temperature fluctuations can be

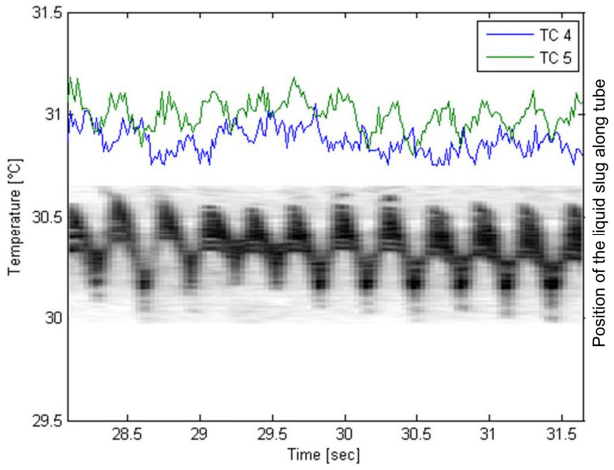

Fig. 8. Correlation between the oscillatory motion of a liquid slug and temperature fluctuations measured by thermocouples TC 4 and TC 5 of the small-scale reference OHP

used to validate the continuation of oscillatory motions in OHPs used in solar water heaters.

It is worth noting that not all thermocouples display noticeable temperature fluctuations, even when liquid slugs are clearly oscillating near the locations where the thermocouples are attached. This can be explained by the difference in time scales between fluid motion and thermal response. The thermocouples are mounted on the outer surface of the OHP tube, while the fluid oscillates inside the tube. When a liquid slug passes by, it can alter the internal wall temperature, but it takes a finite amount of time for this heat to conduct through the tube wall and reach the outer surface where the thermocouple senses it.

If the oscillatory motion is very fast, the liquid slug may move away before enough heat is transferred to the outer wall. In such cases, the thermocouple cannot respond quickly enough to capture each individual temperature change caused by a passing slug. Instead, it may register only a smoothed average or appear as if no fluctuation is occurring. This mismatch between the fluid dynamics time scale and the thermal response time of the system explains why some thermocouples do not reflect the internal oscillation behavior, even though it is physically taking place. Therefore, in this study, thermocouples TC 4 and TC 5 were selected for analysis because they exhibited clear, periodic thermal responses that correlate well with the observed slug oscillation.

Fig. 9 (a) shows the time-series temperature data recorded by thermocouples TC 5, TC 6, TC 9, and TC 11. Two specific time intervals are highlighted with red and blue rectangles. The red rectangle marks a period before oscillatory motion begins, while the blue rectangle indicates a period during which oscillatory motion is present. Fig. 9 (b) presents a closer look at these two intervals. The plots on the left correspond to the red rectangle in Fig. 9 (a) and represent the temperature behavior during non-oscillatory conditions. During this period, the temperatures show a gradual increase with no clear periodic pattern—only random fluctuations are observed. In contrast, the plots on the right in Fig. 9 (b) correspond to the blue rectangle in Fig. 9 (a), where oscillatory motion is active. These graphs show clear periodic temperature fluctuations, indicating that oscillatory heat transfer mechanisms are occurring and sustained during this phase.

This suggests that periodic temperature fluctuations observed in small-scale OHPs can also be detected

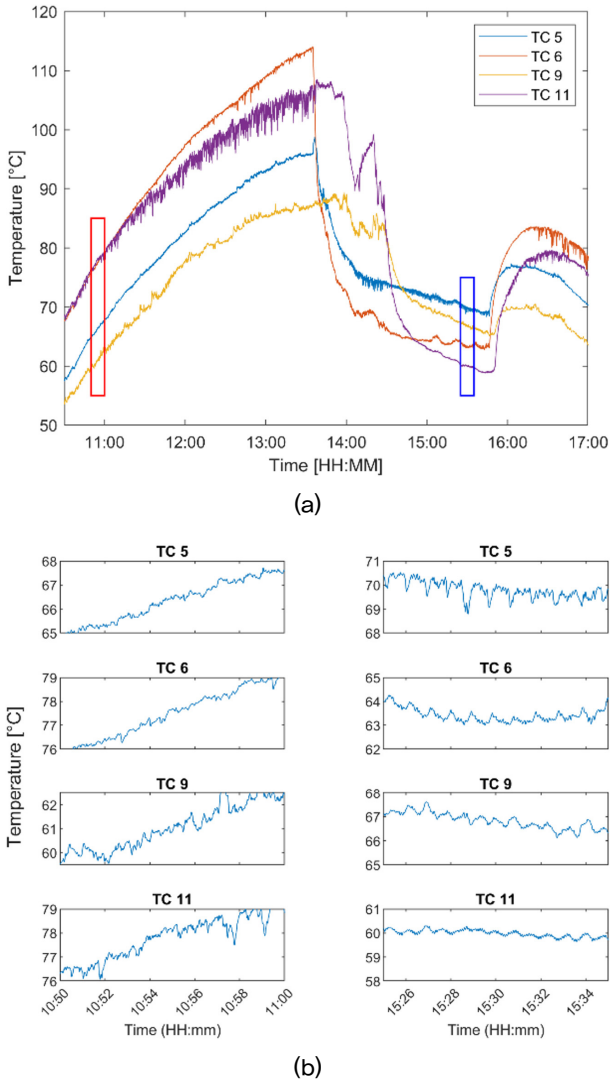

Fig. 9. (a) Time-series temperature data. (b) Enlarged views of the two time intervals marked by the red and blue rectangles in (a). The plots in the left column correspond to the red-highlighted interval (around 11:00), while those in the right column correspond to the blue-highlighted interval (around 15:30).

in the OHPs used in solar water heaters. Therefore, periodic temperature fluctuations can be used to validate the continuation of oscillatory motions in OHPs of solar water heaters. However, although OHPs in solar water heaters exhibit periodic temperature fluctuations, their frequencies and amplitudes differ from those observed in small-scale OHPs. Visual observation suggests that the frequency of periodic temperature fluctuations in small-scale OHPs is higher than in solar water heater OHPs, while the amplitudes of small-scale OHPs are smaller compared to those in solar water heater OHPs. This may be due to differences in liquid slug sizes—since liquid slugs in the solar water heater OHPs are larger than those in small-scale OHPs, they may oscillate more slowly. This finding is important for OHP design in solar water heaters. A larger evaporator area provides an advantage by collecting more solar energy, but it may also result in slower oscillatory motion, which could negatively impact heat transfer efficiency from the evaporator to the condenser. Therefore, future studies should focus on determining the optimal size of OHPs to ensure frequent oscillatory motion of liquid slugs and enhance heat transfer efficiency.

3.4 Thermal resistance

Fig. 10 shows thermal resistance of OHPs for panel B and C for four selected days, which was determined using the following equation,

$$R = \frac{T_e - T_c}{q} \tag{3}$$

The heat transfer rate, q, used in this equation was determined using Equation (2) under the assumption that the heat absorbed in the evaporator flows to the condenser, and then to the heat exchanger without loss. This assumption is considered reasonable due to the insulation of the solar collector, which minimizes heat losses to the surroundings. The four days were

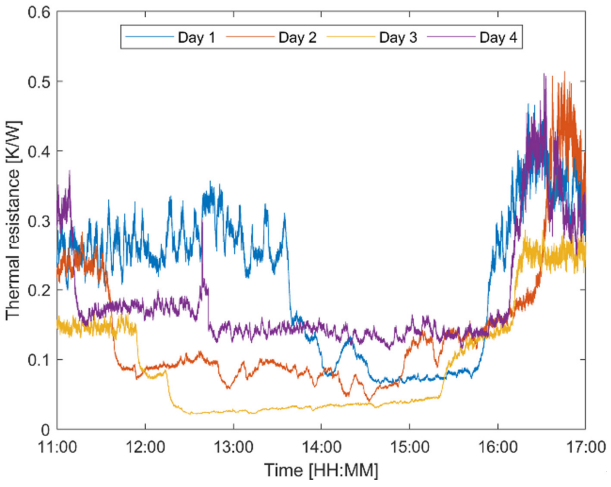

Fig. 10. Thermal resistance of the OHPs in the solar water heater for selected days

chosen from a dataset because they exhibited clear and distinct patterns of evaporator temperature drop, which supports the idea that sudden temperature reductions in the evaporator can be used to identify the onset of oscillating motion. On all selected days, a distinct pattern is observed where thermal resistance decreases suddenly during the midday to early afternoon hours, generally between 11:00 and 14:00, and increases again later in the afternoon. This trend is explained by the onset of oscillating motion within the OHP. When oscillation begins, the oscillatory motion of liquid slugs enhances heat transport efficiency. As a result, the evaporator temperature drops suddenly, leading to a smaller temperature difference across the system. Since thermal resistance is defined as the ratio of temperature difference to heat input, this drop in temperature difference leads to a corresponding sudden decrease in thermal resistance, indicating improved thermal performance. From the observation of the thermal resistance, a sudden drop of thermal resistance can be used as a method to validate the onset and continuation of oscillatory motion in an OHP.

The primary aim of this study is not to evaluate the frequency or statistical occurrence of oscillation, but rather to propose a validation method for detecting

the onset and continuation of oscillating motion in large-scale OHPs used in solar water heaters. Based on observations of the relationship between temperature changes and neutron imaging data, a sudden drop in evaporator temperature consistently appears when oscillating motion begins and continues. Therefore, days that showed this clear temperature response were chosen to illustrate how temperature behavior can be used as an indicator of oscillation. Data without such behavior were excluded, not to disregard contrary results, but because they did not involve the onset of oscillation and were therefore outside the scope of the validation method being proposed in this study.

3.5 Effect of operating and environmental parameters on system performance

Fig. 11 and Fig. 12 show the efficiency distributions with respect to solar irradiance and ambient temperature over three testing days. Each data point represents an individual efficiency value, categorized into four conditions:

(1) no oscillatory motion,

(2) oscillatory motion in panel B only,

(3) oscillatory motion in panel C only, and

(4) oscillatory motion in both panels B and C.

"No oscillatory motion" refers to the absence of oscillation in the OHPs in both panels B and C. "Oscillatory motion in panel B only" and "oscillatory motion in panel C only" indicate that oscillation occurred exclusively in the OHP of panel B or C, respectively. "Oscillatory motion in both panels B and C" indicates that oscillatory motion occurred in the OHPs of both panels simultaneously. Data from panel A were excluded due to a malfunction of its OHP. While the solar irradiance data shown in Fig. 11 was collected every second, the ambient temperature was measured every 5 minutes, which make the plotted data points look less dense compared to the ones shown in Fig. 11.

The data in Fig. 11 clearly show that system efficiencies differ significantly depending on the presence of oscillatory motion. When no oscillatory motion is observed, the efficiency remains below 20% regardless of solar irradiance. In contrast, when oscillatory motion occurs in both panels B and C, efficiency is overall higher than in cases where motion is present only in panel B or C. This indicates that the initiation and maintenance of oscillatory motion are critical for achieving desirable performance in this system. Therefore, future studies are recommended to identify the factors that initiate and sustain oscillatory motion in OHPs

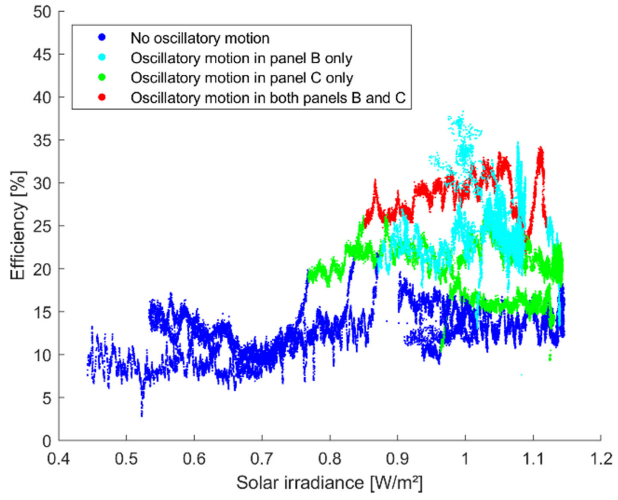

Fig. 11. Efficiency distributions with respect to solar irradiance

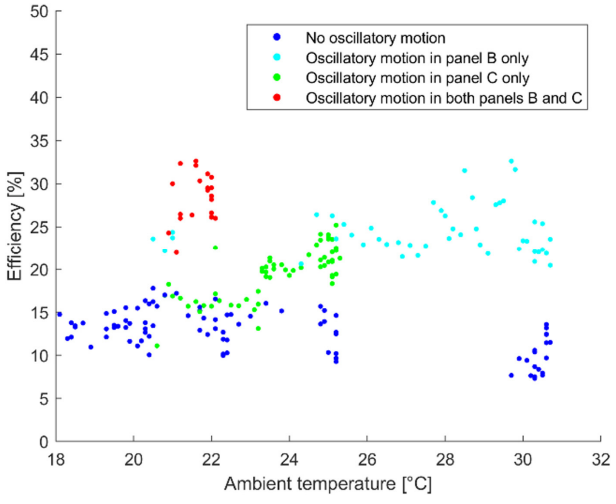

Fig. 12. Efficiency distributions with respect to ambient temperature

when applied to solar water heating systems.

Notably, some outliers in Fig. 11 reach up to 38% efficiency when oscillatory motion occurs in panel B only. These high values coincide with sudden drops in solar irradiance, likely due to passing clouds, and are therefore considered temporary anomalies rather than representative system behavior. Interestingly, at a solar irradiance of approximately 1.1 W/m^2, the efficiency during oscillatory motion in both panels B and C is lower than that in panel B only, which appears counterintuitive. This can be explained using the data in Fig. 12. It shows that the ambient temperature under dual-panel motion was around 21–22°C, while it was significantly higher (28–30°C) during B-only motion. The lower ambient temperature leads to greater heat loss from the system to the environment, reducing thermal efficiency further. This indicates that, in addition to initiating and sustaining oscillatory motion, improving insulation is critical to maximizing the efficiency of this system.

Fig. 13 shows the efficiency distributions with respect to wind speed over three testing days. Wind speed was recorded every 5 minutes. When oscillatory motion occurs only in panel B, the wind speed ranges from approximately 1.5 m/s to 4.2 m/s. Although higher wind speeds are generally expected to reduce efficiency due to increased convective heat loss, the data in this figure show no significant variation in efficiency with wind speed in this range. A similar trend is observed for data points with oscillatory motion in both panels B and C, where the wind speed ranges from 0 to 1.4 m/s. There is no clear relationship between efficiency and wind speed. These results suggest that, within the observed wind speed range of 0 to 4.2 m/s, wind speed does not significantly influence the efficiency of the current system.

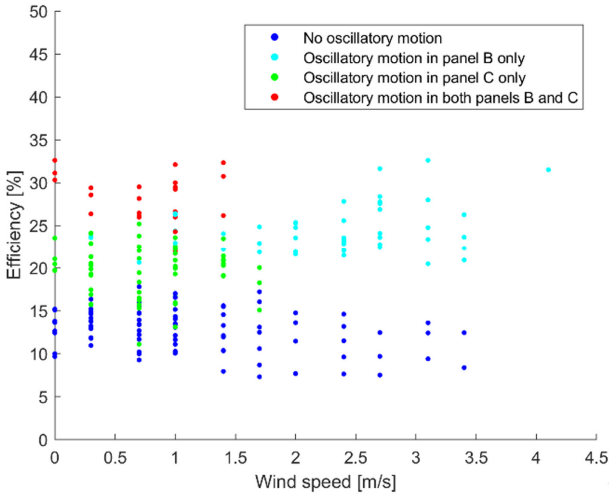

Fig. 13. Efficiency distributions with respect to wind speed

3.6 Onset and continuation of oscillatory motion vs. environmental parameters

This study demonstrates that the onset and continuation of oscillatory motion in oscillating heat pipes (OHPs) are critical for achieving optimal system performance. Therefore, it is important to study the factors that influence this behavior. Oscillatory motion is affected by various factors, including but not limited to vapor pressure inside the OHP tubing, filling ratio, and OHP geometry. However, these aspects are beyond the scope of this study, as their mechanisms are complex and not yet fully understood. As a result, only environmental parameters were considered. Specifically, solar irradiance, ambient temperature, and wind speed were examined to identify potential correlations with the occurrence of oscillatory motion in this system.

Fig. 14 presents the average values of these parameters on days when oscillatory motion either did or did not occur. While it is generally expected that higher solar irradiance would promote oscillatory motion, the data do not consistently support this. In particular, Group B, where oscillatory motion did not occur, exhibits higher average irradiance than Group C, where it did occur—contradicting this expectation. A likely explanation involves ambient temperature. As observed in this study, higher ambient temperatures improve system efficiency by reducing heat loss. Group C shows consistently higher ambient temperatures than Group B, which may have made it easier for

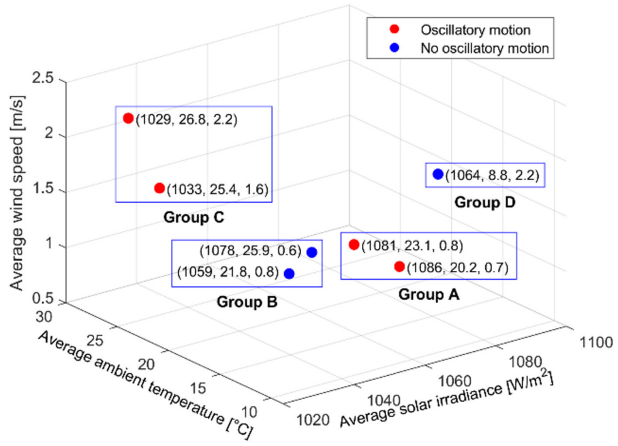

Fig. 14. Onset and continuation of oscillatory motion Vs. environmental parameters

oscillatory motion to start and persist. Group D supports this pattern as well: although it had the highest solar irradiance of all cases, no oscillatory motion was observed, possibly due to its exceptionally low ambient temperature. Wind speed, on the other hand, appears to have little influence.

Group C exhibits higher average wind speeds than Group B, yet still experienced oscillatory motion. This aligns with the earlier finding that wind speed does not significantly impact system efficiency. It is important to emphasize that these findings are specific to the data and configuration of this particular system. They should not be generalized to other OHP designs or operational contexts without further validation.

3.7 Efficiency comparison with a flat plate collector and an evacuated tube collector

Fig. 15 shows the instantaneous efficiency of the solar water heater on a testing day when the OHPs in both panel B and panel C exhibited oscillatory motion and environmental parameter data were available. The data shown corresponds to the efficiency values in Fig. 7 (a), but is limited to the time range from 14:40 to 15:40. This specific time window was selected because both OHP panel B and panel C exhibited oscillatory behavior during this period. It may be argued that the selected time span highlights only the best performance, as it captures a period when the OHP panels were fully active. However, the purpose of Fig. 15 is not to show peak efficiency, but to illustrate the relationship between efficiency (y-axis) and reduced temperature difference (x-axis) in a system that fundamentally relies on OHP-induced oscillatory heat transfer. Therefore, including data from periods without oscillatory motion would misrepresent the actual operating behavior of the OHP-based system.

A study reports the instantaneous efficiencies of flat plate and evacuated tube collectors for both summer and winter conditions.[32] Although a direct, side-by-side comparison of their efficiencies with one of the system used in this study is not possible, a brief comparison is summarized in Table 2. The OHP-based collector's efficiency range (30-40%) falls within the overall ranges reported for both flat plate (20-60%) and evacuated

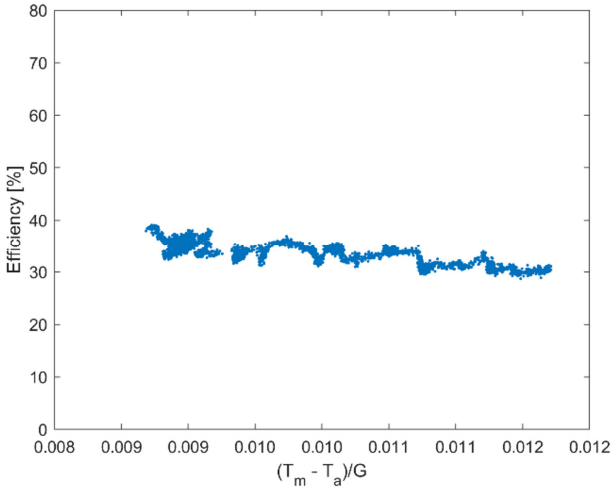

Fig. 15. Instantaneous efficiency of the solar collector utilizing OHPs

Table 2. A brief comparison of efficiencies[32]

Collector Type	Season	Efficiency [%]	Operating Range [℃]
OHP-based	Fall	30-40	0.0087-0.0117
Flat Plate	Winter	20-52	0.033-0.066
Evacuated Tube	Winter	20-48	0.026-0.064
Flat Plate	Summer	30-60	0.024-0.055
Evacuated Tube	Summer	26-54	0.031-0.062

tube collectors (20–54%). However, its operating range is low compared to the others. This suggests that the temperature difference between the fluid and ambient air was relatively small, or the system was tested under relatively high solar irradiance. Due to the limited availability of detailed data from the referenced study, the underlying cause cannot be identified in the present study. Further experimental and comparative analysis is recommended to clarify this issue.

3.8 Repeatability

To evaluate the repeatability of the sudden temperature drops, multiple experiments were conducted across different days. Fig. 16 shows the temperature changes of the evaporators for panel B and panel C on four selected days during which temperature drops were observed. panel B exhibits a sudden temperature drop only on Day 1, whereas panel C shows such drops on all selected days. This suggests that the temperature drops caused by the onset of oscillatory motion are repeatable events, rather than isolated occurrences.

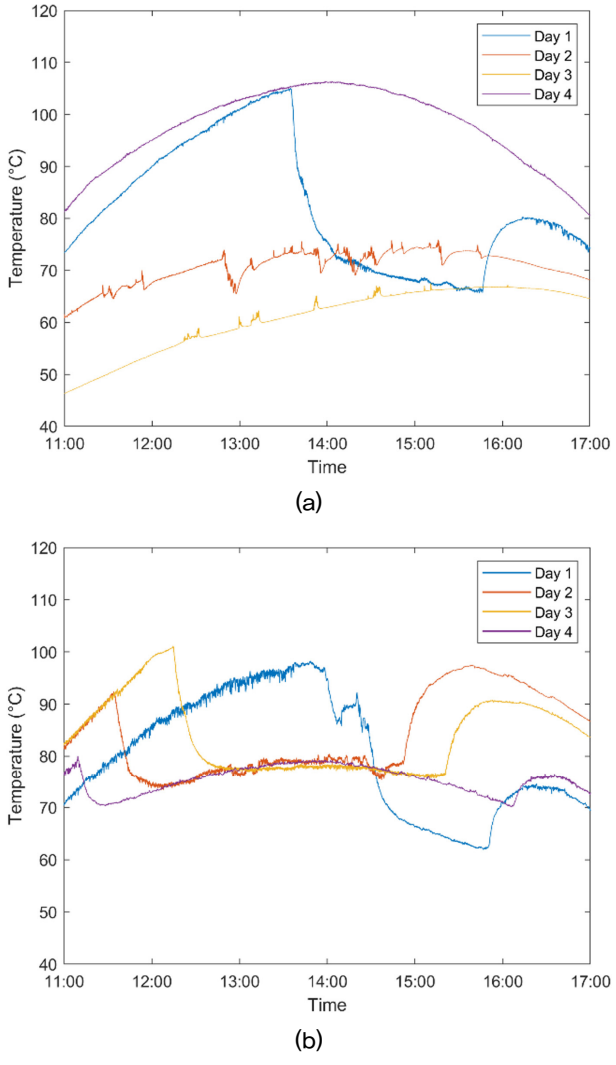

Fig. 16. Average temperatures of the evaporators for panel B in (a) and panel C in (b) on four selected days

The reason why panel B does not exhibit sudden temperature drops on Days 2, 3, and 4, while panel C does, remains unclear. This implies that panel B did not experience the onset or sustained oscillatory motion on those days. The initiation and continuation of oscillatory motion in an OHP are complex phenomena, and the underlying mechanisms are not yet fully understood.[3] Therefore, this issue is beyond the scope of the present study, though it is considered a valuable topic for future research.

3.9 Future studies

As oscillatory motions are the key factor in achieving high performance in solar water heaters with OHPs, it is important to initiate oscillatory motions and maintain them. The onset of oscillatory motion depends on pressure differences between vapor plugs or temperature differences between an evaporator and a condenser. In experimental environments for testing, conditions such as ambient temperature, heat input, and light intensity can be controlled. Under such conditions, the onset of oscillatory motion can be readily achieved by supplying higher heat input to the evaporator and improving cooling at the condenser. However, solar water heaters in actual field applications cannot have controlled conditions. The working conditions of OHPs in solar water heaters vary depending on weather conditions such as solar intensity, ambient temperature, and wind speed. This means that initiating and maintaining oscillatory motions can be

challenging due to uncontrollable weather conditions. Therefore, it is important to study under what weather conditions, such as solar intensity, ambient temperature, and wind speed, oscillatory motions are readily initiated and maintained in future research.

Another suggestion for future study is to visualize oscillatory motions in the OHPs of the solar water heaters used in this study. Although the three validation methods proposed in this study can successfully indicate the onset and continuation of oscillatory motions in OHPs by comparing neutron image data of small-scale OHPs, the oscillatory motions in the OHPs of the solar water heater in this study have not been visually confirmed. Therefore, it is important to visualize the oscillatory motions of liquid slugs using non-destructive techniques such as neutron imaging in future studies.

4. Conclusions

While OHPs are considered promising devices for enhancing the performance of solar water heaters, it is important to validate whether oscillatory motion begins and persists in OHP tubes, as performance heavily depends on the oscillating motion of the working fluid. Due to the relatively large scale of OHPs used in solar water heaters, direct visualization of oscillatory motion is challenging.

In this study, three methods are proposed to validate the onset and continuation of oscillatory motion in large-scale OHPs used in solar water heaters.

1. A sudden temperature drop or cessation of temperature increase in the evaporator indicates the onset of oscillatory motion.
2. A sudden increase in efficiency of an OHP also signals the onset of oscillatory motion.
3. Periodic temperature fluctuations on the surface of OHPs indicate the continuation of oscillatory motion.

This study confirms that the onset and continuation of oscillatory motion are critical for achieving optimal system performance. In addition, solar *irradiance* and ambient temperature are identified as key environmental factors influencing both efficiency and oscillatory behavior.

For future studies, it is recommended to study the effects of weather conditions, such as solar intensity, ambient temperature, and wind speed, on the initiation and stability of oscillatory motion more extensively. Additionally, further research should focus on visualizing the oscillatory motion of liquid slugs in OHPs using non-destructive techniques, such as neutron imaging.

Acknowledgments

This research was supported by the Regional Innovation System & Education (RISE) initiative, funded by the Ministry of Education and administered by the National Research Foundation of Korea (NRF). This article is based in part on the author's Ph.D. dissertation.

References

[1] Lim, H., Yoon, K., Jang, H., and Kim, D., 2007, "Analysis of World's PV Visions 2030", New. Renew. Energy, **3**(1), 5-12.

[2] Su, Z., Hu, Y., Zheng, S., Wu, T., Liu, K., Zhu, M., and Huang, J., 2023, "Recent Advances in Visualization of Pulsating Heat Pipes: A Review", Appl. Therm. Eng., **221**, 119867. https://doi.org/10.1016/j.applthermaleng.2022.119867.

[3] Ma, H., 2015, "Oscillating Heat Pipes", Springer, New York.

[4] Wang, W.-W., Zhang, H.-L., Song, Y.-J., Song, J.-W., Shi, D.-K., Zhao, F.-Y., and Cai, Y., 2022, "Fluid Flow and Thermal Performance of the Pulsating Heat Pipes

Facilitated with Solar Collectors: Experiments, Theories and GABPNN Machine Learning", Renew. Energy, **200**, 1533-1547. https://doi.org/10.1016/j.renene.2022.10.062.

[5] Aref, L., Fallahzadeh, R., Shabanian, S. R., and Hosseinzadeh, M., 2021, "A Novel Dual-Diameter Closed-Loop Pulsating Heat Pipe for a Flat Plate Solar Collector", Energy, **230**, 120751. https://doi.org/10.1016/j.energy.2021.120751.

[6] Charoensawan, P., Wilaipon, P., and Seehawong, N., 2021, "Flat Plate Solar Water Heater with Closed-Loop Oscillating Heat Pipes", Therm. Sci., **25**(5 Part A), 3607-3614. https://doi.org/10.2298/TSCI200713192C.

[7] Winarta, A., Putra, N., Koestoer, R. A., Pamitran, A. S., and Hakim, I. I., 2019, "Experimental Investigation of a Large Scale-Oscillating Heat Pipe at Different Inclinations", Int. J. Technol., **10**(2), 258-268. https://doi.org/10.14716/ijtech.v10i2.2667.

[8] Zhao, J., Jiang, W., and Rao, Z., 2018, "Operational Characteristics of Oscillating Heat Pipe with Long Heat Transport Distance for Solar Energy Application," Exp. Therm. Fluid Sci., **98**, 137-145. https://doi.org/10.1016/j.expthermflusci.2018.05.026.

[9] Gao, Y., Gao, C., Xian, H., and Du, X., 2018, "Thermal Properties of Solar Collector Comprising Oscillating Heat Pipe in a Flat-Plate Structure and Water Heating System in Low-Temperature Conditions", Energies, **11**(10), 2553. https://doi.org/10.3390/en11102553.

[10] Xu, R. J., Zhang, X. H., Wang, R. X., Xu, S. H., and Wang, H. S., 2017, "Experimental Investigation of a Solar Collector Integrated with a Pulsating Heat Pipe and a Compound Parabolic Concentrator", Energy Convers. Manag., **148**, 68-77. https://doi.org/10.1016/j.enconman.2017.04.045.

[11] More, D. A., Pachghare, P. R., and Tech, M., 2016, "Experimental Analysis of Solar Water Heater Using Pulsating Heat Pipe", Int. J. Trend Res. Dev., **3**(3), 482-485.

[12] Kim, J. S., Ha, S. J., Lee, S. I., and Jeong, B. H., 2013, "The Study of Evacuated Solar Collector Using Pulsating Heat Pipe", Front. Heat Pipes, **3**(4). https://doi.org/10.5098/fhp.v3.4.3002.

[13] Yang, Y., Xian, H., Liu, D., Chen, C., and Du, X., 2009, "Investigation on the Feasibility of Oscillating-Flow Heat Pipe Applied in the Solar Collector", Int. J. Green Energy, **6**(5), 426-436. https://doi.org/10.1080/15435070903227896.

[14] Rittidech, S., Donmaung, A., and Kumsombut, K., 2009, "Experimental Study of the Performance of a Circular Tube Solar Collector with Closed-Loop Oscillating Heat-Pipe with Check Valve (CLOHP/CV)", Renew. Energy, **34**(10), 2234-2238. https://doi.org/10.1016/j.renene.2009.03.021.

[15] Rittidech, S., and Wannapakne, S., 2007, "Experimental Study of the Performance of a Solar Collector by Closed-End Oscillating Heat Pipe (CEOHP)", Appl. Therm. Eng., **27**(11-12), 1978-1985. https://doi.org/10.1016/j.applthermaleng.2006.12.005.

[16] Bao, K., Liu, Y., Yan, Y., Ye, G., and Han, X., 2023, "Partial Visualization Study on Flow, Startup and Heat Transfer Characteristics of Closed-Loop Pulsating Heat Pipe with R1336mzz(Z)", Appl. Therm. Eng., **226**, 120218. https://doi.org/10.1016/j.applthermaleng.2023.120218.

[17] Patel, V. M., and Mehta, H. B., 2019, "Channel Wise Displacement-Velocity-Frequency Analysis in Acetone Charged Multi-Turn Closed Loop Pulsating Heat Pipe", Energy Convers. Manag., **195**, 367-383. https://doi.org/10.1016/j.enconman.2019.05.014.

[18] Liu, X., Sun, Q., Zhang, C., and Wu, L., 2016, "High-Speed Visual Analysis of Fluid Flow and Heat Transfer in Oscillating Heat Pipes with Different Diameters", Appl. Sci., **6**(11), 321. https://doi.org/10.3390/app6110321.

[19] Rittidech, S., and Sangiamsuk, S., 2012, "Internal Flow Patterns on Heat Transfer Performance of a Closed-Loop Oscillating Heat Pipe with Check Valves", Exp. Heat Transf., **25**(1), 48-57. https://doi.org/10.1080/08916152.2011.559568.

[20] Wilson, C., Borgmeyer, B., Winholtz, R. A., Ma, H. B., Jacobson, D., and Hussey, D., 2011, "Thermal and Visual Observation of Water and Acetone Oscillating Heat Pipes", J. Heat Transf., 133(6), 061502. https://doi.org/10.1115/1.4003546.

[21] Borgmeyer, B., Wilson, C., Winholtz, R. A., Ma, H. B., Jacobson, D., and Hussey, D., 2010, "Heat Transport Capability and Fluid Flow Neutron Radiography of Three-Dimensional Oscillating Heat Pipes", J. Heat Transf., **132**(6), 061502. https://doi.org/10.1115/1.4000750.

[22] Bhuwakietkumjohn, N., and Rittidech, S., 2010, "Internal Flow Patterns on Heat Transfer Characteristics of a Closed-Loop Oscillating Heat-Pipe with Check Valves Using Ethanol and a Silver Nano-Ethanol Mixture", Exp. Therm. Fluid Sci., **34**(8), 1000-1007. https://doi.org/10.1016/j.expthermflusci.2010.03.003.

[23] Lips, S., Bensalem, A., Bertin, Y., Ayel, V., Romestant, C., and Bonjour, J., 2010, "Experimental Evidences of Distinct Heat Transfer Regimes in Pulsating Heat Pipes (PHP)", Appl. Therm. Eng., **30**(8-9), 900-907. https://doi.org/10.1016/j.applthermaleng.2009.12.020.

[24] Soponpongpipat, N., Sakulchangsatjaati, P., Kammuang-Lue, N., and Terdtoon, P., 2009, "Investigation of the Startup Condition of a Closed-Loop Oscillating Heat Pipe", Heat Transf. Eng., **30**(8), 626-642. https://doi.org/10.1080/01457630802656876.

[25] Kim, J. S., Bui, N. H., Kim, J. W., Kim, J. H., and Jung, H. S., 2003, "Flow Visualization of Oscillation Characteristics of Liquid and Vapor Flow in the Oscillating Capillary Tube Heat Pipe", KSME International Journal, **17**(10), 1507-1519.

[26] Tong, B. Y., Wong, T. N., and Ooi, K. T., 2001, "Closed-Loop Pulsating Heat Pipe", Appl. Therm. Eng., **21**(18), 1845-1862. https://doi.org/10.1016/S1359-4311(01)00063-1.

[27] Yoon, I., Wilson, C., Borgmeyer, B., Winholtz, R. A., Ma, H. B., Jacobson, D. L., and Hussey, D. S., 2012, "Neutron Phase Volumetry and Temperature Observations in an Oscillating Heat Pipe", Int. J. Therm. Sci., **60**, 52-60. https://doi.org/10.1016/j.ijthermalsci.2012.05.004.

[28] Yoon, I., Winholtz, R., and Hongbin Ma, 2023, "Study of Fluid Motions and Thermal Performance of Water and Acetone Oscillating Heat Pipes Using Neutron Imaging", Heat Trans. Res., **55**(5), 23-39. https://doi.org/10.1615/HeatTransRes.2023049240.

[29] Ayel, V., Slobodeniuk, M., Bertossi, R., Romestant, C., and Bertin, Y., 2021, "Flat Plate Pulsating Heat Pipes: A Review on the Thermohydraulic Principles, Thermal Performances and Open Issues", Appl. Therm. Eng., **197**, 117200. https://doi.org/10.1016/j.applthermaleng.2021.117200.

[30] Sugimoto, K., Kamata, Y., Yoshida, T., Asano, H., Murakawa, H., Takenaka, N., and Mochiki, K., 2009, "Flow Visualization of Refrigerant in a Self-Vibration Heat Pipe by Neutron Radiography", Nucl. Instrum. Methods Phys. Res. A: Accel. Spectrom. Detect. Assoc. Equip., **605**(1-2), 200-203. https://doi.org/10.1016/j.nima.2009.01.154.

[31] Tiwari, G. N., 2002, "Solar Energy: Fundamentals, Design, Modelling and Applications", Alpha Science International, Pangbourne, UK.

[32] Lee, S. S., Lim, H. W., Lee, W. J., Lee, K. H., and Shin, U. C., 2024, "On-Site Thermal Performance Evaluation of Flat Plate and Evacuated Tube Solar Collectors", J. Korean Solar Energy, **44**(5), 11-22. https://doi.org/10.7836/kses.2024.44.5.011.